

# Deactivation and regeneration of titanium silicalite catalyst for epoxidation of propylene

Qingfa Wang<sup>\*</sup>, Li Wang, Junxia Chen, Yulong Wu, Zhentao Mi

Key Laboratory for Green Chemical Technology of the Ministry of Education, School of Chemical Engineering & Technology, Tianjin University, Tianjin 300072, PR China

Received 2 October 2006; received in revised form 22 March 2007; accepted 23 March 2007  
Available online 30 March 2007

## Abstract

Continuous epoxidation of propylene with 30-wt% hydrogen peroxide in isopropyl alcohol solvent over titanium silicalite (TS-1) zeolite was carried out and the good selectivity to propylene oxide and stability of TS-1 were obtained. After the reaction of 263 h, the deactivation of the TS-1 catalyst occurred. The spent catalysts were regenerated by calcinations at 550 °C for 5 h, washing with isopropyl alcohol solvent or washing with dilute hydrogen peroxide, and the activity evaluation of the regenerated catalysts were studied. The deactivated and regenerated catalysts were characterized by scanning electron microscopy, X-ray diffraction, Fourier-transform infrared spectroscopy, <sup>29</sup>Si magic angle spinning nuclear magnetic resonance, thermogravimetric analysis and Brunauer–Emmett–Teller method. The compositions deposited on the surface of the catalysts were collected by solvent extraction and were analyzed by gas chromatography–mass spectrometry (GC–MS). The results showed that calcination and washing with dilute hydrogen peroxide were highly effective regeneration methods and the catalytic activity of TS-1 catalysts can be mostly recovered after these treatments. Washing with isopropyl alcohol had a subtle effect in recovering the catalytic activity of the TS-1 catalyst. The major cause of the deactivation of the TS-1 catalyst for epoxidation is blocking micropores induced by bulky organic by-products formed by consecutive reactions of target reaction, such as dimerization or oligomerization of propylene oxide, etherification of propylene oxide with isopropyl alcohol. In addition, leaching of framework titanium also contributes to the deactivation of the catalyst.

© 2007 Elsevier B.V. All rights reserved.

**Keywords:** Propylene epoxidation; Titanium silicalite; Deactivation and regeneration; Blocking; Ti leaching

## 1. Introduction

Propylene oxide (PO) is one of the most important chemical intermediates for producing polyether polyol polymers, such as polyurethane. The commercial chlorohydrin and Halcon routes have many disadvantages in view of environmental and economic considerations. On the other hand, the epoxidation of propylene with hydrogen peroxide using TS-1 catalyst is an environmentally friendly alternative route. Under mild conditions and in methanol medium, a high selectivity of transformation to PO at a relatively high conversion of propylene can be achieved [1]. However, the relatively high cost of the commercial hydrogen peroxide is an obstacle for the commercialization of epoxidation of propylene with hydrogen peroxide

to form PO. The method for resolving this problem is to integrate this process with hydrogen peroxide production. Direct oxidation of propylene with hydrogen and oxygen is an interesting approach [2–8], but a proper multicomponent catalyst, the crucial technique for this integrated process, had not yet been found. As an alternative, the integration of propylene epoxidation by hydrogen peroxide and the formation of hydrogen peroxide by oxidation of secondary alcohols with oxygen is an effective method [9–13]. Among the secondary alcohols, isopropyl alcohol is proper for hydrogen peroxide production. But, it is not known whether isopropyl alcohol is proper as solvent for the epoxidation of propylene over the TS-1 catalyst.

Although TS-1 gives excellent catalytic activity of the propylene epoxidation, the deactivation of the catalyst occurs with time on stream [14,15]. Generally, the activity of TS-1 for propylene epoxidation by 30-wt% hydrogen peroxide in methanol medium becomes lower due to titanium leaching from the catalyst structure [16]. In contrast with many research efforts focused on finding out new catalytic applications of this zeolite in the

<sup>\*</sup> Corresponding author. Tel.: +86 22 27408891; fax: +86 22 27402604.

E-mail addresses: [qingfaw@yahoo.com.cn](mailto:qingfaw@yahoo.com.cn) (Q. Wang),  
[wlytj@yahoo.com.cn](mailto:wlytj@yahoo.com.cn) (L. Wang).

recent years, only a few reports on the TS-1 deactivation exist [17]. The methods of generating deactivated TS-1 are mainly focused on: (1) heat treatment at temperatures from 300 to 700 °C in the presence of different media, such as air, vapor and inert gas [18–24]; (2) oxidation by dilute hydrogen peroxide at temperatures below 100 °C [25–27]; (3) extraction by different solvents such as methanol in the temperature range from 140 to 240 °C [28–30].

The aim of this work was to determine the performance of the TS-1 catalyst for epoxidation of propylene to PO by 30-wt% hydrogen peroxide in isopropyl alcohol medium and to investigate the deactivation and regeneration of the spent TS-1 catalyst in order to explore the possibility of the integration process of PO preparation by propylene epoxidation and hydrogen peroxide production by isopropyl alcohol oxidation. To be specific, two objectives are depicted. First, an extended test of propylene epoxidation by hydrogen peroxide in isopropyl alcohol medium up to 260 h is performed over the TS-1 catalyst in a continuous autoclave reactor to examine the catalytic performance. Second, in order to evaluate the regeneration methods and to examine the deactivation causes, the deactivated TS-1 catalysts is regenerated by calcination, washing with isopropyl alcohol or washing with dilute hydrogen peroxide and characterized by scanning electron microscopy (SEM), Brunauer–Emmett–Teller (BET) method, X-ray diffraction (XRD), Fourier-transform infrared spectroscopy (FT-IR),  $^{29}\text{Si}$  magic angle spinning nuclear magnetic resonance ( $^{29}\text{Si}$  MAS NMR) and thermogravimetric analysis (TGA) and the epoxidation reaction over regenerated catalysts performed in a batch reactor. The compositions deposited on the surface of the catalysts were separated by solvent extraction and analyzed by gas chromatography–mass spectrometry (GC–MS).

## 2. Experimental

### 2.1. Catalyst preparation

TS-1 zeolite was synthesized according to the procedure described in Ref. [31]. One hundred grams of tetraethyl orthosilicate were stirred under  $\text{N}_2$  atmosphere and 3 g of tetraethyl titanate was added followed by dropwise addition of 160 g of a 25 wt% solution of tetrapropylammonium hydroxide. After the alcohol had been evaporated off at 80 °C, 175 g of distilled water was added to the solution. The mixture was transferred to an autoclave, heated at 170 °C under autogeneous pressure for 3 days. After cooling down to room temperature, the crystalline product was separated from the liquid by centrifugation, washed with water, dried at 120 °C for 12 h, and finally calcined at 550 °C for 6 h in air.

### 2.2. Epoxidation procedure, analytical methods and catalyst regeneration

Epoxidation was performed in a stirred autoclave reactor (1000 ml). A ceramic tube was placed on the front of the liquid outlet to separate TS-1 catalyst from the reaction mixture. Twenty grams TS-1 catalyst and 550 ml isopropyl alcohol were

charged into the reactor. The propylene was then fed and the pressure was kept at 0.4 MPa. Then the mixture of isopropyl alcohol and hydrogen peroxide was fed in and out at the flow rate of 120  $\text{ml h}^{-1}$ . In the inlet mixture, the molar ratio of isopropyl alcohol to  $\text{H}_2\text{O}_2$  is 0.5. The reaction temperature was kept at 40 °C and the stirring speed was set at 600 rpm. Samples were withdrawn at different times and immediately injected into a Hewlett-Packard 4890 gas chromatograph with a 15 m HP-5 capillary column (Flame-Ionization Detector). The  $\text{H}_2\text{O}_2$  concentration was determined by iodometric titration.

After the reaction, the spent catalysts were separated by centrifugation and dried at ambient temperature and air, and then regenerated. For the regeneration with isopropyl alcohol or hydrogen peroxide, isopropyl alcohol or 30-wt% hydrogen peroxide was added to a flask containing the spent catalyst. The mixture was stirred for 4.5 h at 80 °C for the regeneration with isopropyl alcohol and 40 °C for the regeneration with hydrogen peroxide. Then the catalysts were separated from the mixture using a centrifuge and dried at 100 °C. For the regeneration by calcinations, the spent catalyst was calcined at 550 °C under air for 5 h.

The catalytic performance of the regenerated samples was tested in a semi-batch autoclave reactor. Isopropyl alcohol (43.2 g), 30-wt% hydrogen peroxide (4.8 g) and TS-1 catalyst (0.7 g) were added to the reactor, and then propylene was fed. The reaction was carried out at 40 °C and 0.4 MPa for 2 h.

### 2.3. Collection and analysis of coke compositions

The coke compositions deposited on the surface of the deactivated catalysts were collected according to Refs. [32,33]. The deactivated catalysts were extracted firstly with carbon tetrachloride and secondly with dichloromethane. Then, the extracted catalyst was dissolved in 40 wt% hydrofluoric acid and the solution thus obtained was extracted by dichloromethane. Finally, three extracts were concentrated by evaporating the solvent and analyzed using a Hewlett-Packard 6890N series gas chromatograph and a 5975 inert mass selective detector, respectively.

### 2.4. Catalyst characterization

XRD patterns were collected on a D/mass-2500 diffractometer using nickel-filtered  $\text{Cu K}\alpha$  radiation ( $\lambda = 0.1540 \text{ nm}$ ). Bragg angles between 5° and 50° were scanned with 0.02° step. FT-IR spectra were recorded at room temperature with a Nicolet Magna-IR 560 spectrometer using the KBr wafer technique. The crystal size was determined by SEM with a JEOL JSM-6400 microscope. TGA analysis was performed on a TA-50 Shimadzu Thermogravimetric Analyzer to study the mass loss of the catalysts under oxygen at flow rate of 20  $\text{ml min}^{-1}$ . The temperature was ramped from 20 °C up to 700 °C at a heating rate of 15 °C  $\text{min}^{-1}$ . The BET data was obtained with a Micromeritics TriStar 3000 analyzer. The samples were heated under vacuum at 120 °C for 4 h prior to the nitrogen adsorption–desorption experiments.  $^{29}\text{Si}$  MAS NMR spectra were recorded on an InfinityPlus spectrometer at room temperature. The parameters of

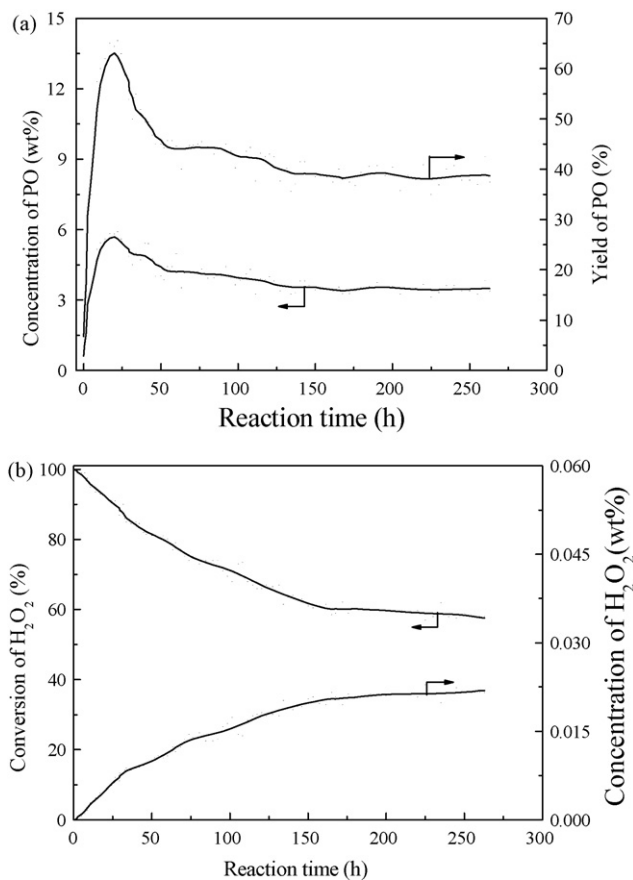


Fig. 1. Continuous epoxidation results of propylene with H<sub>2</sub>O<sub>2</sub> over the fresh TS-1 catalyst: (a) propylene oxide concentration and yield and (b) H<sub>2</sub>O<sub>2</sub> concentration and conversion.

0.8 s pulse width, 4 s recycle delay and 400–1500 scan number were adopted. The 3-trimethylsilyl propane sulfonic acid Na salt (DSS) was used as the external reference.

### 3. Results

#### 3.1. Catalytic performance for PO synthesis

Fig. 1 shows the TS-1 performance for epoxidation of propylene by H<sub>2</sub>O<sub>2</sub> in the continuous reactor. The yield of PO reaches a plateau at the reaction time of approximately 24 h and then decreases rapidly. The maximum yield of PO was 67%. The relatively stable yield of PO over the TS-1 sample in isopropyl alcohol medium can be obtained after approximately 110 h. However, the yield of PO decreased slowly with increasing reac-

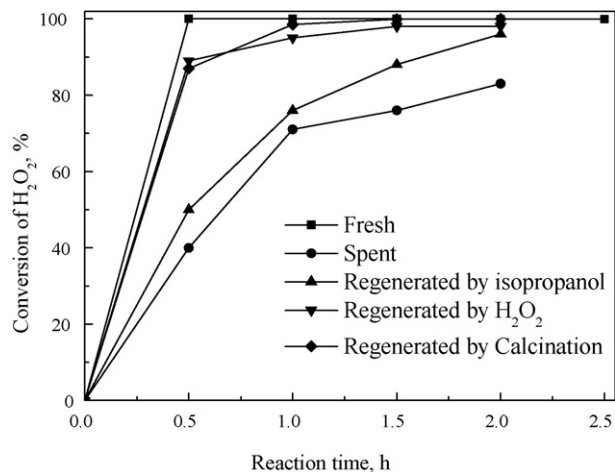


Fig. 2. The H<sub>2</sub>O<sub>2</sub> conversion in catalytic tests.

tion time from 110 to 158 h and then achieved a steady-state up to 263 h again. The stable yield of PO was 43%. Similarly, the high conversion of H<sub>2</sub>O<sub>2</sub> was obtained at initial stages of the reaction because of the high initial activity of TS-1 and the excess amount of propylene in the reaction mixture. Then a decrease in the conversion of H<sub>2</sub>O<sub>2</sub> as a function of time-on-stream up to approximately 158 h was observed. The stable H<sub>2</sub>O<sub>2</sub> conversion of 58% was obtained after approximately 158 h. The TS-1 catalyst thus obtained was the deactivated catalyst.

#### 3.2. Regeneration of the deactivated titanium silicalite catalyst

##### 3.2.1. The catalytic performance of regenerated TS-1 samples

The catalytic performance of regenerated catalysts for the epoxidation of propylene was tested in a batch reactor and the results are presented in Fig. 2. The conversion of H<sub>2</sub>O<sub>2</sub> over the regenerated catalyst by calcination was reduced to 98% of the corresponding fresh catalyst. The conversions of H<sub>2</sub>O<sub>2</sub> obtained on the catalysts regenerated by H<sub>2</sub>O<sub>2</sub>-washing and calcination was similar. The TS-1 catalyst regenerated by isopropyl alcohol washing and the spent TS-1 catalyst were similar in the conversion of H<sub>2</sub>O<sub>2</sub>. The results indicated that calcination and H<sub>2</sub>O<sub>2</sub> washing had a beneficial effect on regenerating the catalytic activity of the spent catalyst, while the regeneration with isopropyl alcohol washing had a subtle effect.

Table 1  
BET results of different TS-1 samples

Samples	Surface area (m <sup>2</sup> g <sup>-1</sup> )	Micropore volume (cm <sup>3</sup> g <sup>-1</sup> )	External surface area (m <sup>2</sup> g <sup>-1</sup> )
Fresh	387.2	0.171	44.6
Calcined	371.4	0.169	44.1
Regenerated with H <sub>2</sub> O <sub>2</sub>	260.2	0.104	39.1
Regenerated with isopropyl alcohol	199.6	0.083	38.9
Deactivated	160.7	0.072	36.4

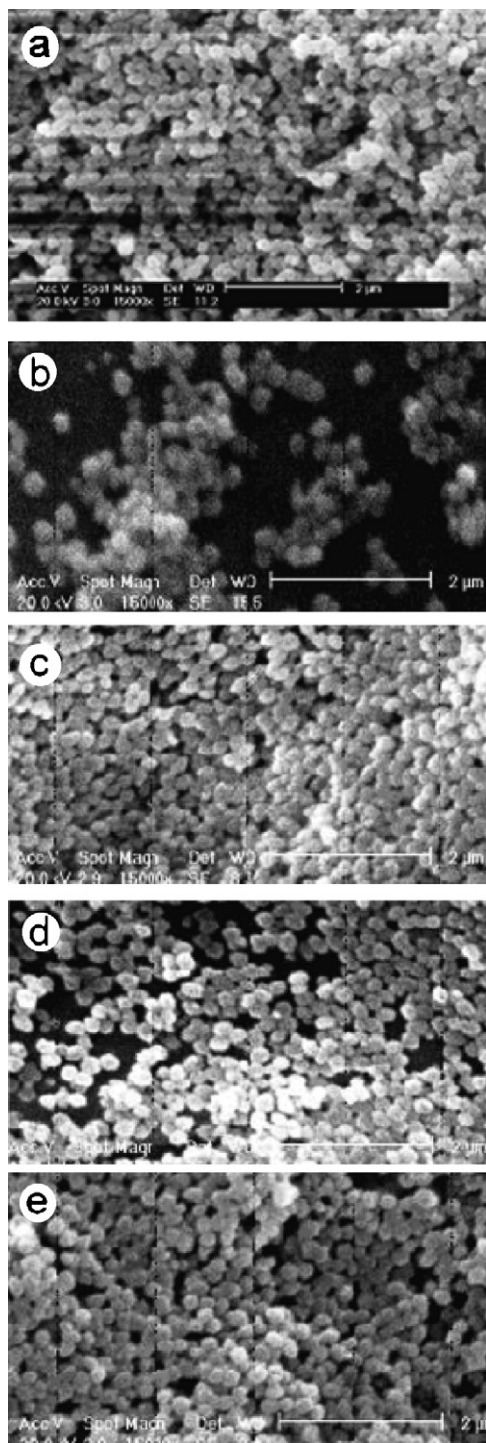


Fig. 3. The SEM micrograph of catalysts: (a) fresh TS-1, (b) deactivation TS-1, (c) regenerated by isopropyl alcohol, (d) regenerated with  $\text{H}_2\text{O}_2$ , and (e) regenerated with calcination.

### 3.2.2. The SEM analysis

The SEM micrographs of the TS-1 samples are shown in Fig. 3. The crystallites of all samples were uniform and their shape showed the typical morphology of the MFI structure. The average crystal size was roughly  $0.2\ \mu\text{m}$ . There is no significant change in the morphology on the spent and regenerated catalysts.

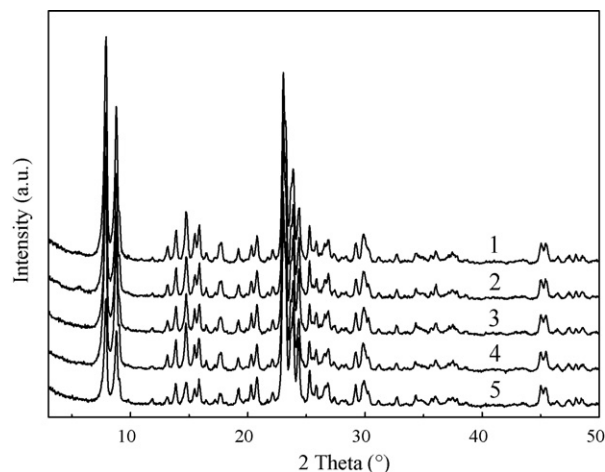


Fig. 4. The XRD pattern of TS-1 catalysts: (1) fresh catalyst, (2) regenerated with isopropyl alcohol, (3) regenerated with  $\text{H}_2\text{O}_2$ , (4) regenerated by calcination, and (5) deactivated catalyst.

### 3.2.3. The BET analysis

The BET results on all catalysts listed in Table 1 have a consistent order with that of hydrogen peroxide conversion in the catalytic tests. The surface area and micropore volume of the deactivated catalyst decreased compared to the fresh sample, indicating majority of the channels of the spent TS-1 catalyst were blocked and the Ti active sites were occupied by the macromolecular by-products. The surface area and micropore volume of the regenerated catalysts increased compared to the spent one and the sample regenerated by calcination gave a relatively high surface area and micropore volume that were close to those of the fresh one.

### 3.2.4. The XRD characterization

The X-ray diffraction patterns of the TS-1 samples are shown in Fig. 4. The main diffraction peaks of all the samples are the same as that of the typical TS-1 zeolite. The single peak at  $2\theta = 24.4^\circ$  indicates a change from monoclinic symmetry (silicate-1) to orthorhombic symmetry (TS-1). The results indicated that the deactivation and regeneration processes had no effect on the crystal structure of TS-1. But there were the significant difference in the crystallinity and unit cell parameters between the fresh and deactivated and regenerated catalysts. The crystallinity of the samples was calculated according to the method described in Ref. [34] and the results are listed in Table 2. The relative crystallinity of the spent catalyst decreased significantly. The relative crystallinity of the regenerated samples was higher than that of the spent one but lower than that the fresh one. It indicated that there were some crystal defects in the regenerated and deactivated samples. These crystal defects may promote the formation of by-products due to its high acidity [35].

The unit cell parameters were calculated using the standard equation for an orthorhombic unit cell [36] and the results are listed in Table 2. The unit cell volumes of the fresh one, regenerated samples by calcination and hydrogen peroxide treatment lie between the values of  $5340\text{--}5405\ \text{\AA}^3$  reported in literature [36]. But, the unit cell volume of the regenerated sample by calcina-

Table 2  
The XRD and FT-IR results of different samples

Samples	Relative crystallinity	Cell parameter (Å)			Unit cell volume (Å <sup>3</sup> )	<i>I</i> <sub>960</sub> / <i>I</i> <sub>550</sub>
		<i>a</i>	<i>b</i>	<i>c</i>		
Fresh	1.00	20.08 (1)	19.92 (2)	13.41 (1)	5373.6 (10)	0.45
Calcined	0.91	20.07 (1)	19.94 (2)	13.42 (1)	5370.1 (10)	0.43
Regenerated with H <sub>2</sub> O <sub>2</sub>	0.90	20.08 (1)	19.85 (2)	13.51 (1)	5384.5 (10)	0.42
Regenerated with isopropyl alcohol	0.89	20.17 (1)	19.94 (2)	13.44 (1)	5407.2 (10)	0.35
Spent	0.78	20.13 (1)	20.02 (2)	13.50 (1)	5439.3 (10)	0.19

tion was lower than that of the fresh one, indicating a decrease in the framework titanium contents on the regenerated catalyst. In contrast, the unit cell volumes of the deactivated catalyst and the catalyst regenerated by isopropyl alcohol treatment were not in the range above.

### 3.2.5. The TGA characterization

TG–DTG curves of the catalysts are shown in Fig. 5. The TS-1 catalyst regenerated by calcination had no weight loss (not shown). The weight loss of the samples increased with decreasing H<sub>2</sub>O<sub>2</sub> conversion in catalytic tests. It is seen that the fresh catalyst has almost no weight loss and the curve is linear. TG–DTG curves of the spent and regenerated catalysts were similar and there were three distinct stages of weight loss in the temperature range of 50–550 °C. Three stages of weight loss are attributed to desorption of water and PO [37,38], the bulky molecular by-products deposited on the surface and channels of TS-1 catalysts, respectively. The weight loss of the spent catalyst at the first stage between 50 and 200 °C was higher than that of the regenerated samples. The weight loss of the H<sub>2</sub>O<sub>2</sub> treatment sample at the third stage between 400 and 550 °C was slightly lower than that of the sample washed with isopropyl alcohol.

### 3.2.6. The FT-IR characterization

Fig. 6 shows the FT-IR spectra of TS-1 catalysts. The main absorption bands are observed at 1230, 1104, 960, 804, 550 and 450 cm<sup>-1</sup>, which agreed with the FT-IR spectra of TS-1 reported

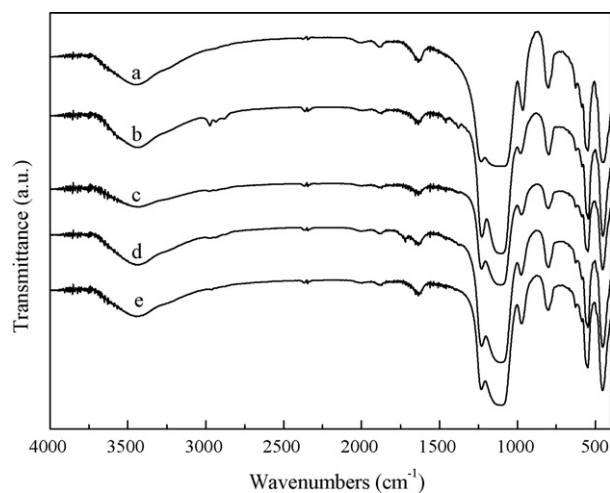


Fig. 6. The FT-IR spectra of TS-1 catalysts: (a) fresh catalyst, (b) spent catalyst, (c) regenerated with isopropyl alcohol, (d) regenerated with H<sub>2</sub>O<sub>2</sub>, and (e) regenerated by calcination.

in the literature [39,40]. The bands at 550 and 800 cm<sup>-1</sup> are assigned to  $\delta(\text{Si-O-Si})$  and  $\nu(\text{Si-O-Si})$ , respectively. It is well known that an absorption band in the 960 cm<sup>-1</sup> is assigned to the stretching mode of the [SiO<sub>4</sub>] tetrahedral bond with Ti atoms and may be considered as the fingerprint of framework titanium. However, such assignment has also been interpreted in term of Si-OH groups and may be considered as a structural defect rather

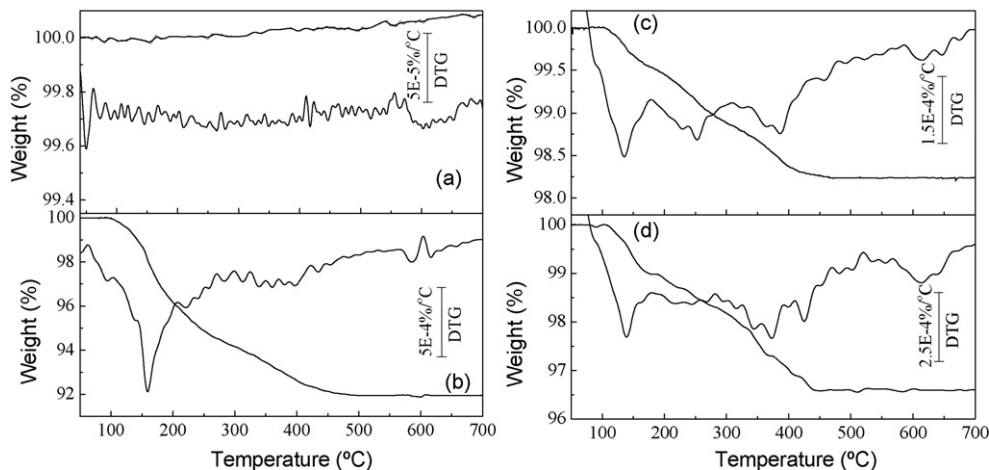


Fig. 5. TG–DTG profiles of catalysts: (a) fresh TS-1, (b) deactivated TS-1 catalyst, (c) TS-1 catalyst regenerated with H<sub>2</sub>O<sub>2</sub>, and (d) the TS-1 catalyst regenerated with isopropyl alcohol.

than an atom isomorphously substituted for silicon in the silica framework [41]. But it is commonly accepted as the characteristic of asymmetry of Ti- and Si-containing zeolites. A strong intensity of band at  $960\text{ cm}^{-1}$  is consistent with a low symmetry of framework structure. The symmetry of framework structure of Ti- and Si-containing zeolites decreases with an increase in the content of Ti [42–45]. Therefore, the decrease in symmetry of framework structure is the indirect evidence of titanium incorporated into the MFI structure. Table 2 summarized the peak area ratio of the band at  $960\text{ cm}^{-1}$  to that of  $550\text{ cm}^{-1}$  ( $I_{960}/I_{550}$ ) in the FT-IR spectra for all samples. It was observed that the peak area ratio for the spent and regenerated catalysts was lower than that for the fresh catalyst. However, the ratio for the catalysts regenerated by calcination and  $\text{H}_2\text{O}_2$  treatment were close to that for the fresh one. The results indicated that there was an irreversible change in the framework symmetry of the TS-1 catalyst during its deactivation process. Table 2 and Fig. 2 show that  $I_{960}/I_{550}$  of all samples was consistent with their conversion of  $\text{H}_2\text{O}_2$  in the catalytic tests. It implies that the irreversible change in the framework symmetry of the TS-1 catalyst for the epoxidation reaction of propylene results in its irreversible deactivation.

For the spent catalyst, it was observed that the peak at  $960\text{ cm}^{-1}$  shifted to  $968\text{ cm}^{-1}$ . This was likely caused by the change of the coordination structure and vibration of Ti(IV) atom induced by the bulky by-products deposited in the channels of the catalyst. Boccuti and his co-workers also found that the peak at  $960\text{ cm}^{-1}$  shifted to higher wave numbers with a significant decrease in the intensity due to the absorption of water or other molecules [46]. In addition, some of stretching bands in the range of  $2900\text{--}3000\text{ cm}^{-1}$  appeared, which can be assigned to the saturated C–H appeared in the FT-IR spectrum of spent catalyst. This revealed that some bulky molecular substances with saturated C–H existed on the spent catalyst. Maybe, etherish species also exist on the catalyst while they could not be authenticated only by FT-IR due to the interference vibration of the Ti–O, Si–O and C–O bond in the TS-1 catalyst.

### 3.2.7. $^{29}\text{Si}$ MAS NMR characterization

Fig. 7 shows the  $^{29}\text{Si}$  MAS NMR spectra of all samples. There are peaks at  $\delta = -113.4\text{ ppm}$  and  $\delta = -116.4\text{ ppm}$  in all spectra. If only the peak at  $\delta = -113.4\text{ ppm}$  appears, the zeolite exhibits monoclinic symmetry. The presence of the  $\delta = -113.4\text{ ppm}$  peak together with the  $\delta = -116.4\text{ ppm}$  shoulder indicates the orthorhombic symmetry of zeolite. The results reported by Thangaraj and co-workers [47] and by Li and co-workers [48] show that S-1 and TS-1 with lower titanium content exhibit monoclinic symmetry at room temperature. With the increase in the framework titanium content, the symmetry of TS-1 structure gradually changes from the monoclinic structure to the orthorhombic structure. Therefore, on the basis of XRD patterns, FT-IR spectra and  $^{29}\text{Si}$  MAS NMR spectra, it is concluded that a significant fraction of titanium in these catalysts is situated in framework positions. Compared to the fresh and regenerated catalysts, an obvious change in chemical shift of two peaks to high-field side was observed in the spectra of the deactivated catalyst. This might be ascribed to the

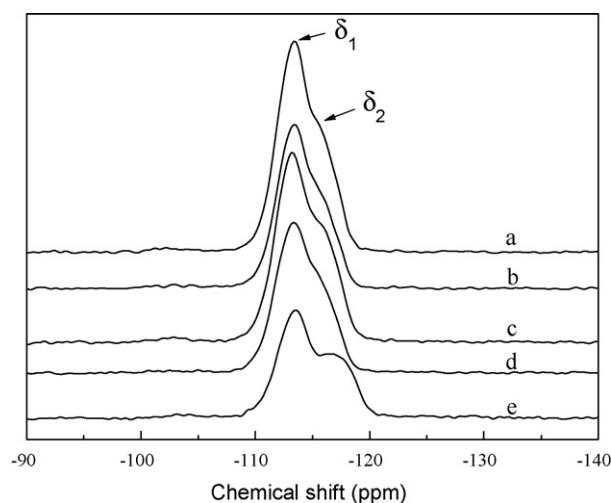


Fig. 7.  $^{29}\text{Si}$  MAS NMR of TS-1 catalysts: (a) fresh, (b) calcined, (c) regenerated with  $\text{H}_2\text{O}_2$ , (d) regenerated with isopropyl alcohol, and (e) deactivated.

more coke components on the deactivated catalyst than on other samples.

## 4. Discussion

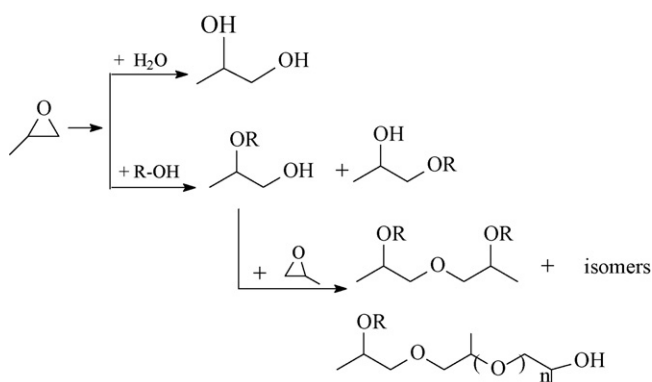
The major product of the epoxidation reaction of olefins with hydrogen peroxide in alcohol medium over the TS-1 catalyst is the corresponding epoxide. Depending on the reaction conditions, the following by-products were obtained in various amounts: diol, ether, organic acid, aldehyde, polymer [1]. Among them, the ether formed by the etherification of epoxide with alcohol is the major by-product. The steric hindrance of isopropyl alcohol to the reaction is more serious than that of methanol. Therefore, the rate of the etherification reaction is slower in isopropyl alcohol than in methanol because the reaction rate of etherification is influenced by the steric hindrance of alcohol to the reaction. It is well known that the rate of the epoxidation reaction of propylene with  $\text{H}_2\text{O}_2$  is significantly influenced by the gas–liquid mass transfer because it is a gas–liquid–solid three-phase reaction. A relatively high solubility of propylene in the liquid medium has a beneficial effect on the epoxidation reaction. However, the solubility of propylene in methanol was lower than that in isopropyl alcohol. Therefore, the high PO yield of epoxidation of propylene with hydrogen peroxide in the isopropyl alcohol medium, which was very close to that in the methanol medium, was obtained although isopropyl alcohol has a serious steric hindrance to epoxidation of propylene than methanol. The results obtained in our work indicated that there is a possibility that the integrated process of propylene epoxidation by  $\text{H}_2\text{O}_2$  and hydrogen peroxide generation by oxidation of isopropyl alcohol are achieved with a relatively high yield of PO and stability of the TS-1 catalysts.

In present work, the coke components deposited on the deactivated catalyst was collected by extraction and analyzed by GC–MS. There were three families of the coke components corresponding to their possible origin (presented in Table 3) except the reactant, solvent and target product in the extracts. But, in the final dichloromethane extract, only the compounds in fam-

Table 3  
Major components of the coke extracted from the deactivated catalyst

Family no.	Molecular weight	Compound	Formula
1	76	1,2-Propanediol	
2	118	Propylene glycol isopropyl alcohol ether	
3	134	Dipropylene glycol	
	176	Dipropylene glycol monoisopropyl alcohol ether	

ilies 1 and 2 were found and the compounds in family 3 were mainly found in the first carbon tetrachloride extract. This result indicated that the compounds in families 1 and 2 deposited in the channels of the deactivated catalyst and the dimeric compounds and oligomers deposited mostly on the external surface of the deactivated catalyst. 1,2-Propanediol and propylene glycol isopropyl ether are formed by hydrolysis of PO and nucleophilic addition of alcohol, respectively, catalyzed by the weak acid Ti-center (see Scheme 1). According to the method of estimating molecular dimension with Materials Studio 3.0 software in Refs. [49,50], the kinetic diameter of propylene glycol isopropyl ether was about  $0.66 \text{ nm} \times 0.51 \text{ nm}$ . The pore size of TS-1 catalyst with an MFI structure are  $0.53 \text{ nm} \times 0.56 \text{ nm}$  for straight channel and  $0.51 \text{ nm} \times 0.55 \text{ nm}$  for the sinusoidal channel [51–53]. Therefore, the hydrolysis and etherification by-products can be formed in the channels and external surface of the catalysts. However, as a result of the channel constraints, the by-products formed by consecutive reactions of etherification reaction can only be formed on the external surface. The molecules of the by-products formed in the micropores of TS-1 cannot diffuse out from the channel of TS-1 immediately and part of them resided in the micropores. As a result of the blockage of the channel, the deactivation phenomenon of the TS-1 catalyst occurred because most of the active Ti-sites located in the channels of TS-1 [47,54,55].



Scheme 1. By-products of propylene epoxidation by  $\text{H}_2\text{O}_2$  over TS-1.

Among the regeneration methods used in our work, isopropyl alcohol washing is a physical separation process and its effect on recovering activity of the deactivated catalyst depends on the resistance of extraction mass transfer and the solubility of the deposits in the alcohol. Therefore, the deposits on the external surface of the catalysts could be removed easily by this method. But, it is difficult to remove the deposits in the micropores of the catalysts, resulting in a relatively low efficiency of the regeneration. The results of our experiments as well as that with refluxing methanol [56,4] well confirmed this. Hydrogen peroxide washing and calcinations at high temperature are chemical reaction processes. The bulky by-products can be oxidized by hydrogen peroxide to form small molecular compounds [57]. The small molecules could easily diffuse out from the micropores of the catalysts. However, minority of bulk by-products might remain in the micropores because of their complete conversion. At high temperatures, the complete oxidation reaction of the organic compounds with oxygen can occur and a result of a full recovery in the activity of the TS-1 catalysts should be attained. But,  $\text{H}_2\text{O}_2$  conversion over this sample was reduced to 98% of the corresponding fresh catalyst. This result indicated that the irreversible deactivation of the TS-1 catalyst occurred in epoxidation process. This might be ascribed to framework titanium leaching caused by the solvolysis of polar molecules such as water and hydrogen peroxide that react with the tetrahedral titanium to form octahedral titanium peroxo-species [56]. In addition, the defects on TS-1 catalyst may also cause titanium leaching from the crystalline structure of TS-1 during reaction [58–60].

## 5. Conclusions

The epoxidation reaction of propylene with hydrogen peroxide over the TS-1 catalyst in the isopropyl alcohol medium can be performed with a high yield of PO and stability of TS-1. The PO yield of 67% and the  $\text{H}_2\text{O}_2$  conversion of 91% were obtained after the reaction of approximately 24 h. The major cause of the deactivation of TS-1 catalysts was the blockage of the TS-1 catalyst channels caused by bulky by-products formed by reacting propylene epoxide with isopropyl alcohol and further

oligomerization. Ti leaching also contributed to the deactivation of TS-1 catalysts. The effectiveness of the regeneration with the isopropyl alcohol treatment was low because this method could only partly remove the deposits in the micropores of TS-1. Both the regeneration methods by calcination and the hydrogen peroxide treatment are very effective in the recovery of the catalytic activity of the TS-1 catalysts, especially the former.

## Acknowledgements

The supports of the National Natural Science Foundation of China (Granted No. G 20446003) and the PhD Specific foundation of the Ministry of Education (Granted No. G 20030056035) for this research are greatly acknowledged.

## References

- [1] A. Wróblewska, E. Ławro, E. Milchert, *Ind. Eng. Chem. Res.* 45 (2006) 7365.
- [2] A. Takahashi, N. Hamakawa, I. Nakamura, T. Fujitani, *Appl. Catal. A: Gen.* 294 (2005) 34.
- [3] B. Taylor, J. Lauterbach, W.N. Delgass, *Appl. Catal. A: Gen.* 291 (2005) 188.
- [4] G. Jenzer, T. Mallat, M. Maciejewski, F. Eigenmann, A. Baiker, *Appl. Catal. A: Gen.* 208 (2001) 125.
- [5] N. Yap, R.P. Andres, W.N. Delgass, *J. Catal.* 226 (2004) 156.
- [6] R. Meiers, U. Dingerdissen, W.F. Hölderich, *J. Catal.* 176 (1998) 376.
- [7] T. Hayashi, K. Tanaka, M. Haruta, *J. Catal.* 178 (1998) 566.
- [8] Y. Liu, K. Murata, M. Inaba, N. Mimura, *Appl. Catal. B: Environ.* 58 (2005) 51.
- [9] G.L. Crocco, J.C. Jubin, J.G. Zajacek, US Patent 5,693,834 (1997), to ARCO Chemical Technology.
- [10] J.C. Jubin, G.L. Crocco, J.G. Zajacek, US Patent 5,523,426 (1996), to ARCO Chemical Technology.
- [11] C. Neril, B. Anfossi, A. Esposito, US Patent 4,833,260 (1989), to Anic.
- [12] J.C. Jubin, US Patent 5,468,885 (1995), to ARCO Chemical Technology.
- [13] J.G. Zajacek, J.C. Jubin, G.J. Crocco, US Patent 5,384,418 (1994), to ARCO Chemical Technology.
- [14] C. Perego, A. Carati, P. Ingallina, *Appl. Catal. A: Gen.* 221 (2001) 63.
- [15] M.G. Clerici, G. Bellussi, U. Romano, *J. Catal.* 129 (1991) 159.
- [16] L. Davies, P. McMorn, D. Bethell, P.C.B. Page, F. King, F.E. Hancock, G.J. Hutchings, *Chem. Commun.* 18 (2000) 1807.
- [17] G.F. Thiele, E. Roland, *J. Mol. Catal. A* 117 (1997) 351.
- [18] G.J. Crocco, J.G. Zajacek, US Patent 5,741,749 (1998), to Arco Chemical Technology.
- [19] J.P. Catinat, M. Strebelle, US Patent 6,169,050 (2001), to Solvay.
- [20] M.A. Mantegazza, US Patent 6,403,514 (2002), to Enichem.
- [21] B. Sun, W. Wu, E. Wang, Y. Li, S. Zhang, L. Hu, US Patent 20,030,228,970 (2003), to China Petroleum & Chemical Corporation.
- [22] H.Z. Han, K.M. Carrol, US Patent 6,872,679 (2005), to Arco Chemical Technology.
- [23] U. Muller, J.H. Teles, A. Wenzel, W. Harder, P. Rudolf, A. Rehfinger, N. Reiber, US Patent 6,790,969 (2004), to BASF.
- [24] G.H. Grosch, U. Muller, A. Walch, N. Reiber, W. Harder, US Patent 6,710,002 (2004), to BASF.
- [25] G. Thiele, US Patent 5,620,935 (1997), to Degussa.
- [26] P. Gilbeau, WO Patent 9,818,555 (1998), to Solvay and Gilbeau Patrick.
- [27] M.A. Mantegazza, L. Balducci, L. Rivetti, US Patent 6,403,514 (2002), to Enichem.
- [28] K.M. Carroll, H.E. Morales, Y.Z. Han, US Patent 5,916,835 (1999), to Arco Chemical Technology.
- [29] D. Shaumont, WO Patent 9,901,445 (1999), to Arco Chemical Technology.
- [30] T. Chang, EP Patent 1,190,770 (2002), to Arco Chemical Technology.
- [31] M. Taramasso, G. Perego, B. Notari, US Patent 4,410,501 (1983), to Snamprogetti.
- [32] S.M. Holmes, A. Garforth, B. Maunders, J. Dwyer, *Appl. Catal. A: Gen.* 151 (1997) 355.
- [33] X. Zhang, Y. Wang, F. Xin, *Appl. Catal. A: Gen.* 307 (2006) 222.
- [34] T.A. Nijhuis, B.J. Huizinga, M. Makkee, J.A. Moulijn, *Ind. Eng. Chem. Res.* 38 (1999) 884.
- [35] M.G. Clerici, U. Romano, US Patent 4,937,216 (1990), to Eniricerche and Enichem Sintesi.
- [36] C.S. Cundy, J.O. Forrest, *Micropor. Mesopor. Mater.* 72 (2004) 67.
- [37] M.A. Uguina, D.P. Serrano, R. Sanz, J.L.G. Fierro, M. López-Granados, R. Mariscal, *Catal. Today* 61 (2000) 263.
- [38] X. Lin, *Catal. Today* 93/94 (2004) 505.
- [39] E. Astorino, J.B. Peri, R.J. Willey, G. Busca, *J. Catal.* 157 (1995) 482.
- [40] T. Armaroli, F. Milella, B. Notari, R.J. Willey, G. Busca, *Top. Catal.* 15 (2001) 63.
- [41] N. Phonthammachai, M. Krissanasaeerane, E. Gulari, A.M. Jamieson, S. Wongkasemjit, *Mater. Chem. Phys.* 97 (2006) 458.
- [42] M.C. Capel-Sanchez, J.M. Campos-Martin, J.L.G. Fierro, *Appl. Catal. A: Gen.* 246 (2003) 69.
- [43] P.F. Henry, M.T. Weller, C.C. Wilson, *J. Phys. Chem. B* 105 (2001) 7452.
- [44] C. Lamberti, S. Bordiga, A. Zecchina, A. Carati, N.F.G. Artioli, G.P.M. Salvalaggio, G.L. Marrak, *J. Catal.* 183 (1999) 222.
- [45] G.L. Marra, G. Artioli, A.N. Fitch, M. Milanesio, C. Lamberti, *Micropor. Mesopor. Mater.* 40 (2000) 5.
- [46] M.R. Boccuti, K.M. Rao, A. Zecchina, *Stud. Surf. Sci. Catal.* 48 (1989) 133.
- [47] A. Thangaraj, R. Kumar, S.P. Mirajkar, P. Ratnasamy, *J. Catal.* 130 (1991) 1.
- [48] G. Li, X. Wang, X. Guo, S. Liu, Q. Zhao, X. Bao, L. Lin, *Mater. Chem. Phys.* 71 (2001) 195.
- [49] E. Xing, X. Zhang, L. Wang, Z. Mi, *Catal. Commun.* 6 (2005) 737.
- [50] Y. Liu, Z. Gao, *Acta Petrol. Sin.* 12 (1996) 35.
- [51] W.M. Meier, D.H. Olson, *Atlas of Zeolite Structure Types*, Butterworth-Heinemann, Stoneham, 1992, p. 138.
- [52] T. Tatsumi, N. Jappar, *J. Catal.* 161 (1996) 570.
- [53] M. Milanesio, G. Artioli, A.F. Gualtieri, L. Palin, C. Lamberti, *J. Am. Chem. Soc.* 125 (2003) 14549.
- [54] S. Ikeda, H. Nur, P. Wu, T. Tatsumi, B. Ohtani, *Stud. Surf. Sci. Catal.* 145 (2002) 251.
- [55] M.G. Clerici, *Top. Catal.* 15 (2001) 257.
- [56] L.Y. Chen, G.K. Chuah, S. Jaenicke, *J. Mol. Catal. A* 132 (1998) 281.
- [57] H. Liu, G. Lua, Y. Guo, Y. Guo, J. Wang, *Chem. Eng. J.* 108 (2005) 187.
- [58] C. Lamberti, S. Bordiga, D. Arduino, A. Zecchina, F. Geobaldo, G. Spano, F. Genoni, G. Petrini, A. Carati, F. Villain, G. Vlaic, *J. Phys. Chem. B* 102 (1998) 6382.
- [59] L. Davies, P. McMorn, D. Bethell, P.C.B. Page, F. King, F.E. Hancock, G.J. Hutchings, *Phys. Chem. Chem. Phys.* 3 (2001) 632.
- [60] L. Davies, P. McMorn, D. Bethell, P.C.B. Page, F. King, F.E. Hancock, G.J. Hutchings, *J. Catal.* 198 (2001) 319.